AL-QADISIYAH JOURNAL FOR ENGINEERING SCIENCES

Vol. 10 , No. 2
ISSN: 1998-4456

ANALYSIS AND SIMULATION OF A TRIPLE-STAGE SERIES FLOW ABSORPTION CHILLER CYCLE FOR AIR CONDITIONING APPLICATIONS

Qusay Rasheed AL-AMIR,

Department of Mechanical Engineering, Babylon University, Hilla, Iraq

Email: qusay1972@gmail.com

Received on 25 January 2017 *Accepted on 6 April 2017*

Abstract: *This paper represents a numerical study of a triple-stage series flow absorption cycle operating with LiBr-H2O pair. A computational model is implemented using Engineering Equation Solver (EES) software. This model includes equations of mass, species and energy conservation. The analysis is used to simulate a triple stage absorption chiller utilization for an air conditioning applications with a nominal capacity of 300kW manufactured by Thermax company. This chiller is indirect fired type which uses steam from boiler of the HPG as heat source. The variations of performance parameters with different ranges of operation conditions have been calculated. The operating parameters are selected as follows: the HPG, MPG and LPG temperatures: THPG= 150-230°C, TMPG= 100-130°C and TLPG= 60-95°C, respectively, LPC temperature TLPC= 28-37°C, evaporator temperature Tevap = 5-14°C; flow rate of refrigerant mr= 1 kg/s; four values of heat exchangers effectiveness 0.4, 0.5, 0.6 and 0.65. In addition, the comparison between the present study and other study obtained in literature review has been done. The analysis revealed that maximum COP is found as a function of both MPG and LPG temperatures. The results outline that the COP increases with an increase in the evaporator and generators temperature but decreases with condenser temperature.*

Keywords: triple-stage LiBr-H2O absorption cycle, EES software, COP, thermodynamic analysis.

Nomenclature		o	Outlet
C	Specific heat capacity (kJ/kg.K)	s	Strong solution
h	Enthalpy [kJ/kg]	r	Refrigerant
m	Mass flow rate [kg/s]	w	Weak solution
p	Pressure(kPa)	Abbreviations	
Q	Heat transfer rate(kW)	COP	Coefficient of performance
T	Temperature (C)	EES	Engineering Equation Solver
f	Circulation ratio(-)	HE	Heat exchanger
W	Work (kW)	H_2O	Water
X	Species concentration	HPC	High-pressure condenser
Greek symbols		HPG	High-pressure generator
ϵ	Effectiveness	LiBr	lithium bromide
Subscripts		LPC	Low-pressure condenser
a	Absorber	LPG	Low-pressure generator

c	Condenser	MPC	Middle-pressure condenser
e	Evaporator	MPG	Middle-pressure generator
g	Generator	SHX	Solution heat exchanger
in	Inlet	TV	Expansion valve

1. INTRODUCTION AND OVERVIEW

The absorption refrigeration is investigated as one of environmentally friendly refrigeration technologies. This technology depends on heat instead of electricity to produce cooling load which is employed for air conditioning purposes or ice making. However, absorption system required to auxiliary accessories to work with high efficiency such as cooling tower to cool the refrigerant in both the condenser and absorber, and low grade heat sources to heat the generator to increase the system performance. Many and various energy sources are used in absorption systems such as solar energy, geothermal, biomass and waste heat from the fossil fuel combustion in industries or power plants.

Absorption chillers utilize a refrigerant–absorbent pair as a working fluid such as water-ammonia, lithium chloride-water, lithium bromide-water and lithium nitrate-ammonia. The most common conventional fluids using for absorption chillers for both cooling and heating applications are water-ammonia and lithium bromide-water due to their have the desirable properties than the other fluids. The absorption chiller also is a closed loop cycle which can be classified into five types such as half-stage, single-stage, double-stage, triple-stage and multi-stage. The single-stage and half-stage chillers operate using low temperature hot water with respect to a double-stage, triple-stage and multi-stage chillers (Chidambaram et al,. 2011). The cycle performance improves more with increasing number of stages but it requires higher temperature waste heat (greater 175C) and extra components. In addition to above, there are also two other absorption chillers which are diffusion absorption and hybrid chillers. These systems give better performance (Ullah et al., 2013).

Several theoretical studies in this field are done on the single-stage (Sencan et al., 2005, Aphornratana and Sriveerakul, 2007, Kim et al., 2009, Bahman, 2011, and Ha, 2013) and double-stage cycles (Misra et al., 2005, Figueredo et al. 2008, Kaushik and Arora, 2009, Marcos et al., 2011). For instance, Saghiruddin and Siddiqui, 2001 conducted economic analysis and thermodynamic of the single effect absorption cycle. They used various working fluid in their analysis such as NH3-H2O, LiBr-H2O, NH3-LiNO3 and NH3-NaSCN and different sources of energy such as solar collectors, LPG and Biogas. Grossman and Zaltash, 2001 have made a computer ABSIM code for the flexible and modular form simulation of a single-effect absorption schemes with different working fluids. Joudi and Lafta, 2001 offered a computational model to describe the influence of several operating cases on the function of each component and to find the single-effect absorption refrigeration system performance working on LiBr–H2O solution. Florides et al., 2003 formed a mathematical model based on balance of mass and energy equations written for each components of absorption cycle with 1 kW cooling capacity. Mehrabian and Shahbeik, 2005 developed the computer study for a single-effect absorption chiller using solution consisted of lithium bromide and water as a working fluid. The program provides the thermodynamic properties of all state points and the overall cycle performance. Gomri, 2009 has conducted the comparative study between single-effect and double-effect absorption refrigeration systems. The results of their study showed there is minor difference between the exergetic efficiency of the system as well as the COP of double-effect system is about twice the COP of single-effect system. Somers et al., 2011 designed a numerical study using ASPEN for single- and double-effect water/lithium bromide absorption chiller. Predictions for the single and double-effect designs were within 3% and 5%, respectively for all absorption cycle parameters. Wardono and Nelson, 1996 carried out a system optimization for a double-effect lithium bromide absorption chiller driven by hot water based on the steady simulation of the chiller.

Further triple-stage cycle studies have also been conducted for instance Gomri, 2008. He used exergy analysis to simulate a triple effect vapor absorption system at various operation conditions.. He calculated the exergy loss of each component of cycle and concluded that the maximum value of exergetic efficiency

AL-QADISIYAH JOURNAL FOR ENGINEERING SCIENCES

Vol. 10 , No. 2
ISSN: 1998-4456

for the triple effect refrigeration system was about 35.1 % and the temperature of low pressure generator was more important than the temperature of middle-pressure generator. He also showed that the maximum exergy and COP were found for a maximum value of low pressure generator and middle-pressure generator temperatures. As well as Azhar and Siddiqui, 2013 conducted a comparison study between triple effect absorption cycle and both of the single and double effect cycles. Economic analysis and performance parameters were also investigated in their paper. They concluded that the triple effect cycle is more economical and more efficient than that of single and double effect cycles. In addition, the triple effect absorption cycle can required high temperature heat sources, therefore liquefied petroleum gas (LPG) and compressed natural gas (CNG) were the best choice for operating the triple effect LiBr-H2O absorption systems.

A little studies is mentioned in open literature about simulate of the triple-stage series flow absorption cycles because the cycle analysis is somewhat complex. Therefore, this paper is concentrated on developing a computer program to simulate of the this cycle and simulation results is validated with actual absorption chiller cycle based on a 300 kW cooling capacity. The current study is capable to evaluate the performance of a triple-stage series flow absorption cycle working with LiBr-H2O pair under different operating conditions.

2. CHILLER DESCRIPTION AND WORKING PRINCIPLE

Triple-stage absorption chiller usually constructs from an ordinary double-stage absorption chiller with an added high-pressure generator (HPG). A photograph of the triple-stage absorption chiller using LiBr–H_2O solution are showed in figure 1.

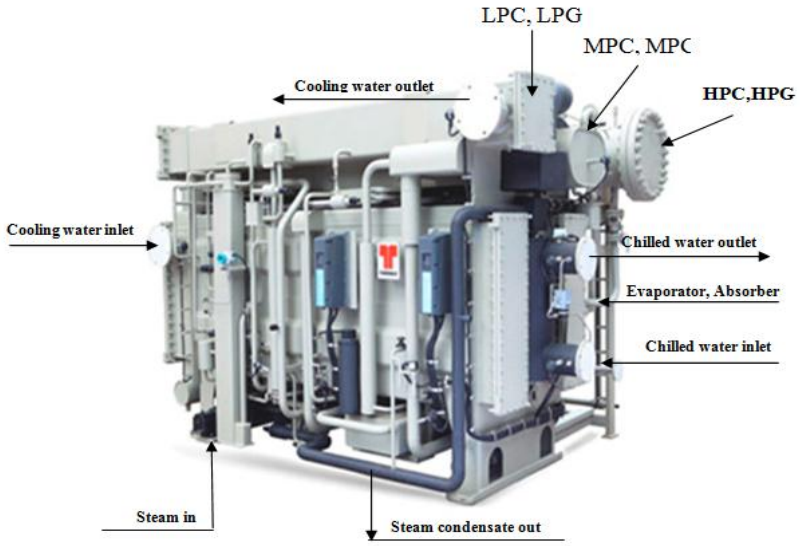

Figure 1. Three-stage steam-fired chiller system (Source)

It constructs from three generators (a high-pressure generator (HPG), a middle-pressure generator (MPG), and a low-pressure generator (LPG)), three condensers (a high-pressure condenser (LPC), a middle-pressure condenser (MPC), and a low-pressure condenser(LPC) or main condenser), solution pump, three solution heat exchangers (HX1, HX2, and HX3), absorber, evaporator, and six throttling valves (TV1,TV2,TV3,TV4,TV5, and TV6). These components are connected in three closed loops and also connected with auxiliary systems as depicted in figure 2.

AL-QADISIYAH JOURNAL FOR ENGINEERING SCIENCES

Vol. 10 , No. 2

ISSN: 1998-4456

These loops are as following: the first loop with low pressure consisted from generator (LPG), condenser(LPC), solution pump, solution heat exchanger(HE1), absorber, evaporator, and solution and refrigerant throttling device(TV1 and TV6). The second loop with medium pressure consisted from generator (MPG), condenser (MPC), solution heat exchanger (HX2), solution and refrigerant throttling device (TV2, TV5). When the final loop with high pressure consisted from generator (HPG), condenser (MPG), solution heat exchanger (HX3), solution and refrigerant throttling device (TV3, TV4). On the other side, the auxiliary systems connect to chiller system which are as following:

1- Indirect-fired system connected with HPG to heat and maintain hot water supply temperature,

2- Cooling tower system to cool the refrigerant for both the LPC and absorber which is installed outer surface of the buildings,

3- System consisted of storage tank and air-handling unit to conditioning space below ambient conditions which is typically installed outside the buildings.

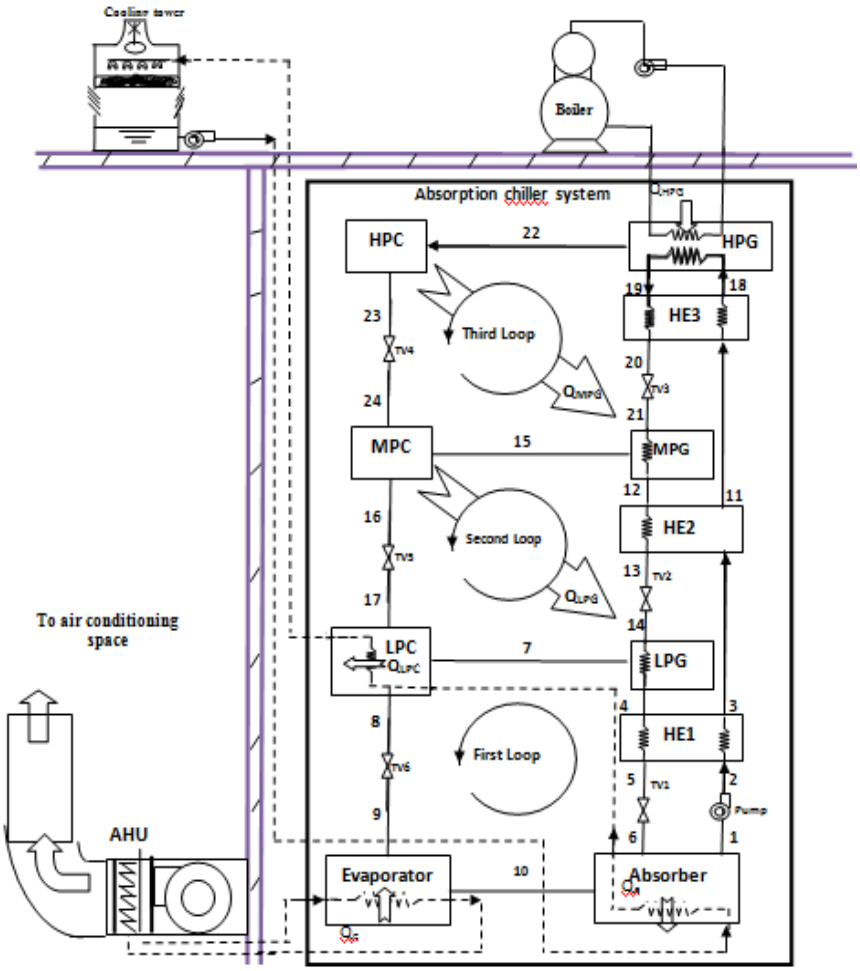

Figure 2. State points of triple-stage LiBr-H_2O absorption chiller system connected with auxiliary system

AL-QADISIYAH JOURNAL FOR ENGINEERING SCIENCES

Vol. 10 , No. 2

ISSN: 1998-4456

In this cycle, the solution exiting the absorber at state point 1 is first impelled to the HPG through three heat exchangers (i.e. HE1, HE2 and HE3). At the HPG, the heat energy from an external heat source extracts the refrigerant vapor (water) from the solution. The refrigerant vapor in superheated state is then passed to the HPC at state point 22 and condenses into liquid releasing its heat. At this condenser, the condensation heat of refrigerant vapor is used to heat the MPG. The remaining solution, called strong solution leaving the HPG at state point 19, where flows through the heat exchanger (HE3) and the reducing valve (TV3) towards the MPG at state point 21. In the MPG, some vapor is generated that enters the MPC at state point 15. The condensation heat in MPC is used to heat the LPG. The concentrated solution which is leaving the MPG at state point 12, then flows through heat exchanger (HE2) towards the LPG at state point 14. More refrigerant is generated in LPG that enters the LPC at state point 7 from which heat is transferred to the cooling water flowing through the LPC. Hence, the refrigerant which is entered in the LPC represents overall refrigerant coming from the three generators. The condensed refrigerant leaves the LPC and flows through the expansion valve (TV6) to reduce it pressure and enters to the evaporator at state point 9 and starts to boil after taking heat from the water circulated between the evaporator and the conditioning space. The vaporization heat of the refrigerant produces the cooling capacity of the whole system. The refrigerant vapor in the evaporator flows back into the absorber at state point 10 where it absorbs by the strongest solution coming from the LPG at state point 6. The cycle then gets completed.

MATHEMATICAL MODELING

Some assumptions are made to simplify the model:

1- The cycle model is based on steady state analysis,

2- Flow configuration is series, where the weak solution is pumped directly from absorber to HPG,

3- The Lithium bromide solution at the outlet of generators is weak solution and strong solution at the outlet of the absorber.

4- The pressure inside each condenser equals to that in each the generator,

5- The pressure inside the evaporator equal to the absorber ,

6- The flow through throttling valves are isenthalpic,

7- The vapor produced in the MPG, HPG and evaporator is superheated,

8- The solution of LiBr/water is saturated at outlet of both the LPG and the absorber

9- The diluted solution pumped by the solution pump from the absorber to the HPG has constant mass flow rate.

10- The exit temperature different between the MPC and LPG is equal to 5K

11- The exit temperature different between the HPC and MPG is equal to 5K

12- The refrigerant leaving the LPC is at the same temperature as the solution in the absorber exit.

13- The heat transfer at the HPC equals to the heat transfer at the MPG. While the heat transfer at the MPC equals to the heat transfer at the LPG.

The general equations of these principles are specified as:

Mass balance

$$\sum \dot{m}_{in} = \sum \dot{m}_{out} \qquad (1)$$

Species balance

$$\sum(mX)_{in} = \sum(m\dot{X})_{out} \quad (2)$$

Energy balance

$$\sum\dot{Q} + \sum\dot{W} + \sum\dot{m}_{in} h_{in} - \sum\dot{m}_{out} h_{out} = 0 \quad (3)$$

The circulation ratio (*f*) is defined as the ratio of weak solution flow rate to refrigerant flow rate. This parameter is very important for system design and is given by:

$$f = \frac{\dot{m}_w}{\dot{m}_r} \quad (4)$$

Or it is expressed by terms of concentrations as

$$f = \frac{X_{gen,out}}{X_{gen,out} - X_{abs,out}} \quad (5)$$

The cooling mode coefficient of performance (COP_c) for absorption chiller cycle is given by the following formula.

$$COP_c = \frac{chiller\ load}{Energy\ \ input} = \frac{Q_e}{Q_{HPG} + W_p} \quad (6)$$

The refrigerant leaves the evaporator as saturated vapor at state point 10. The enthalpy is expressed by (ASHRAE fundamentals, 2009)

$$h_{sat} = -0.00124397 \times T_{evap}^2 + 1.88060937 \times T_{evap} + 2500.559 \quad (7)$$

On the other hand, the refrigerant vapor leaves both HPG and MPG at stat points 22 and 15 as superheated vapor, respectively. The enthalpy is expressed by (Hosseini, 2011)

$$h_{\sup} = 1.925 \times T_{gen} - 0{,}125 \times T_{cond} + 2365 \quad (8)$$

COMPONENT ANALYSIS

The cycle was treated as an independent element for each component with a certain number of input values. The components of triple stage absorption chiller with their state points can be depicted in figure 2. The components are: (1) condenser. (2) Refrigerant expansion valve. (3) Solution expansion valve, (4)

AL-QADISIYAH JOURNAL FOR ENGINEERING SCIENCES

Vol. 10 , No. 2
ISSN: 1998-4456

Evaporator, (5) Absorber, (6) Solution pump, (7) Solution heat exchanger, (8) Generator. The mass, species and energy equations can be applied to each components of absorption cycle as shown in Table 1.

Table 1: Summary of equations for each component of the cycle

Components	Mass and spices balances	Energy balance	State points
Absorber	$m_1 = m_{10} + m_6$, $X_1 m_1 = X_6 m_6$	$Q_a = m_{10}h_{10} + m_6 h_6 - m_1 h_1$	1, 6, 10
Solution pump	$m_1 = m_2 = m_{18}$ $X_1 = X_2$	$W + m_1 h_1 = m_2 h_2$ $W_{pump} = m_1(h_2 - h_1)$	1, 2
LPC	$m_8 = m_{17} + m_7$	$Q_{LPC} + m_8 h_8 = m_{17}h_{17} + m_7 h_7$ $Q_{LPC} = m_{17}h_{17} + m_7 h_7 - m_8 h_8$	7, 8, 17
MPC	$m_{16} = m_{24} + m_{15}$	$Q_{MPC} + m_{16}h_{16} = m_{15}h_{15} + m_{24}h_{24}$ $Q_{MPC} = m_{15}h_{15} + m_{24}h_{24} - m_{16}h_{16}$	15,16 , 24
HPC	$m_{23} = m_{22}$	$Q_{HPC} + m_{23}h_{23} = m_{22}h_{22}$ $Q_{HPC} = m_{22}h_{22} + m_{23}h_{23}$	22 , 23
TV1,TV2, TV3	$m_5 = m_6$, $m_{13} = m_{14}$, $m_{20} = m_{21}$	$h_5 = h_6$, $h_{13} = h_{14}$, $h_{20} = h_{21}$	5,6,13,14,20,21
TV4,TV5, TV6	$m_{23} = m_{24}$, $m_{16} = m_{17}$, $m_9 = m_8$	$h_{23} = h_{24}$, $h_{16} = h_{17}$, $h_9 = h_8$	9,8,16,17,23, 24
HE1	$m_2 = m_3$, $m_4 = m_5$	$Q_{HE1} = m_1(h_3 - h_2) = m_4(h_4 - h_5)$	2, 3, 4, 5
HE2	$m_3 = m_{11}$, $m_{12} = m_{13}$	$Q_{HE2} = m_{12}(h_{12} - h_{13}) = m_3(h_{11} - h_3)$	3, 11, 12, 13
HE3	$m_{11} = m_{18}$, $m_{19} = m_{20}$	$Q_{HE3} = m_{11}(h_{18} - h_{11}) = m_{19}(h_{20} - h_{19})$	11, 18, 19 , 20
LPG	$m_{14} = m_4 + m_7$ $X_{14}m_{14} = X_4 m_4$	$Q_{LPG} + m_{14}h_{14} = m_7 h_7 + m_4 h_4$ $Q_{LPG} = m_7 h_7 + m_4 h_4 - m_{14}h_{14}$	4, 7, 14
MPG	$m_{21} = m_{15} + m_{12}$ $X_{21}m_{21} = X_{12}m_{12}$	$Q_{MPG} + m_{21}h_{21} = m_{15}h_{15} + m_{12}h_{12}$ $Q_{MPG} = m_{15}h_{15} + m_{12}h_{12} - m_{21}h_{21}$	12, 15, 21
HPG	$m_{18} = m_{22} + m_{19}$ $X_{18}m_{18} = X_{19}m_{19}$	$Q_{HPG} + m_{18}h_{18} = m_{22}h_{22} + m_{19}h_{19}$ $Q_{HPG} = m_{22}h_{22} + m_{19}h_{19} - m_{18}h_{18}$	18, 19, 22
Evaporator	$m_r = m_9 = m_{10}$	$Q_e + m_9 h_9 = m_{10}h_{10}$ $Q_e = m_r(h_{10} - h_9)$	9, 10
Other parameters			
Heat exchanger effectiveness for HE1, HE2 and HE3			
HE1	$\varepsilon_{HE1} = \frac{(T_4 - T_5)}{(T_4 - T_2)}$		2, 4, 5
HE2	$\varepsilon_{HE2} = \frac{(T_{12} - T_{13})}{(T_{12} - T_3)}$		3,12, 13
HE3	$\varepsilon_{HE3} = \frac{(T_{19} - T_{20})}{(T_{19} - T_{11})}$		11,19,20
Circulation ratio for LPG, MPG, HPG			
LPG	$f_{LPG} = \frac{m_{14}}{m_7} = \frac{X_4}{X_4 - X_{14}}$		4,7,14
MPG	$f_{MPG} = \frac{m_{21}}{m_{15}} = \frac{X_{12}}{X_{12} - X_{21}}$		12,15, 21
HPG	$f_{HPG} = \frac{m_{18}}{m_{22}} = \frac{X_{19}}{X_{19} - X_{18}}$		18,19, 22

AL-QADISIYAH JOURNAL FOR ENGINEERING SCIENCES

Vol. 10 , No. 2
ISSN: 1998-4456

MODEL VALIDATION

The available data in the literature were used to validate the simulation results. The theoretical results done by Gomri, 2010 for the triple-stage absorption cycle are used. The comparative variation of the COP value with generator temperature is highlighted in Figure 3. Good agreements were observed between the present results and the presented by Gomri, 2010.

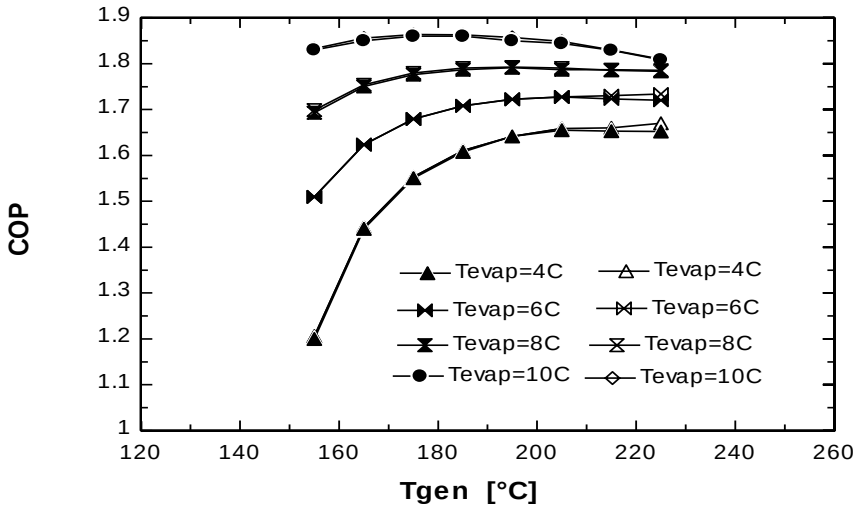

Figure 3. Comparison of COP between the percent study (right legend) and Gomri 2010 (left legend) at different generator exit temperature.

SIMULATION MODEL

In this study, a computational program is carried out using EES software (Klein, 2009). This program is based on equations of mass and heat balances for the thermodynamic properties of lithium bromide–water. Simulation of three-stage indirect-fired absorption chiller cycle includes inputs and outputs. The inputs of the system include the evaporator exit temperature, LPC exit temperature, HPG exit temperature, mass flow rate of refrigerant, effectiveness of heat exchangers. The outputs include the enthalpies, mass flow rates, LiBr concentrations, temperatures and pressures at each state points as well as cooling capacity, circulation ratio, heat transfer rates, coefficient of performance (COP).

The three-stage indirect-fired absorption chiller manufactured by Thermax company had a rated capacity of 300 kW and COP of 1.8 at design conditions. According to the Eq. 6, the energy input to the chiller should not be excess 166 kW under rating conditions.The original chiller cycle can be worked effectively at 180°C HPG exit temperature, 30°C LPC exit temperature, 5°C evaporator exit temperature, 1 kg/s refrigerant mass flow rate, 0.65 heat exchanger effectiveness. Under these operating conditions, the output parameters (temperature, pressures, vapor quality, flow rate, concentration and concentration) and various state points (1-24) are delineated in Table 2. The performance parameters results and heat transfer rates generated by EES for absorption chiller cycle are reported in Table 3.

RESULTS AND DISCUSSION

The variation in the results also are carried out for different ranges of operating conditions. Exit temperature is varied in the following range: HPG temperature THPG= 150-230°C, MPG temperature

AL-QADISIYAH JOURNAL FOR ENGINEERING SCIENCES

Vol. 10 , No. 2
ISSN: 1998-4456

TMPG= 100-130°C and LPG temperature TLPG= 60-95°C, LPC temperature TLPC = 28-37°C, and evaporator temperature Te = 5-14°C. Mass flow rate of refrigerant is mr = 1.0 kg/s. Heat exchangers effectiveness are 0.4, 0.5, 0.6 and 0.65

Table 2:The computed state point results of the cycle.

State points	Temperature(C)	Pressure (kpa)	Quality Kg/kg	Mass flow rate(kg/s)	Enthalpy kJ/kg	Concentration X(%)
1	30.0	1.60	-	1.000	57.0	46.57
2	30.0	4.25	-	1.000	57.0	46.57
3	47.7	4.25	-	1.000	97.1	46.57
4	69.5	4.25	-	0.8782	166.8	58.65
5	43.8	4.25	-	0.8782	116.3	58.65
6	50.5	1.60	0.0048	0.8782	116.3	58.65
7	47.5	4.25	-	0.0406	2588.4	-
8	30.0	4.25	-	0.1149	125.7	-
9	5	1.60	0.0271	0.1149	125.7	-
10	5	1.60	-	0.1149	2526.2	-
11	80.2	37.72	-	1.000	171.3	46.57
12	120.8	37.72	-	0.9188	268.0	58.65
13	73.2	37.72	-	0.9188	174.1	58.65
14	69.8	4.25	0.0025	0.9188	174.1	58.65
15	96.2	37.72	-	0.0406	2676.3	-
16	74.5	37.72	-	0.0812	311.8	-
17	30.0	4.25	0.0766	0.0812	311.8	-
18	133.1	238.04	-	1.000	293.7	46.57
19	180.0	238.04	-	0.9594	384.9	58.65
20	125.6	238.04	-	0.9594	277.4	58.65
21	74.4	37.72	0.0372	0.9594	277.4	58.65
22	152.4	238.04	-	0.0406	2770.6	-
23	125.8	238.04	-	0.0406	528.6	-
24	74.4	37.72	0.0934	0.0406	528.6	-

Table 3: The performance parameter results of the cycle.

Parameter	Values
Heat absorber, Q_{abs}(kW)	293.745
Heat evaporator, Q_{evap}(kW)	232.4
Heat generator(LPG), Q_{LPG} (kW)	75.9
Heat generator(MPG), Q_{MPG} (kW)	96.7
Heat generator(HPG), Q_{HPG} (kW)	141.3
Heat condenser(LPC), Q_{LPC}(kW)	80
Heat condenser (MPC), Q_{MPC}(kW)	75.9
Heat condenser(HPC), Q_{HPC}(kW)	96.9
Solution heat exchanger(HX1), Q_{HX1}(kW)	35.1
Solution heat exchanger(HX2), Q_{HE2}(kW)	40.4
Solution heat exchanger(HX3), Q_{HX3}(kW)	27.9
Solution pump, W_p(kW)	0.1527
LiBr strong solution(%X6)	59
LiBr strong solution(%X16)	59.35
LiBr strong solution(%X26)	61.691
COP(-)	1.64

AL-QADISIYAH JOURNAL FOR ENGINEERING SCIENCES

Vol. 10 , No. 2

ISSN: 1998-4456

Figures 4 to 6 show the effect of the HPG, LPG and MPG temperatures, respectively on system COP and solution circulation ratio. These figures also show that the system COP values increase with increase in HPG, LPG and MPG temperatures. As seen in Figure 4, the higher COP is found at HPG temperature of 210°C while the higher COP values are found for a maximum value of MPG and LPG temperatures as shown in Figures 5 and 6 respectively. This temperature represents the optimum HPG temperature. This finding agrees with the results done by Rabah Gomri, 2008. Furthermore, the increase in HPG, LPG and MPG temperatures produces increasing in refrigerant mass flow rate passing through the condensers thus leading to an decrease in the solution circulation ratio.

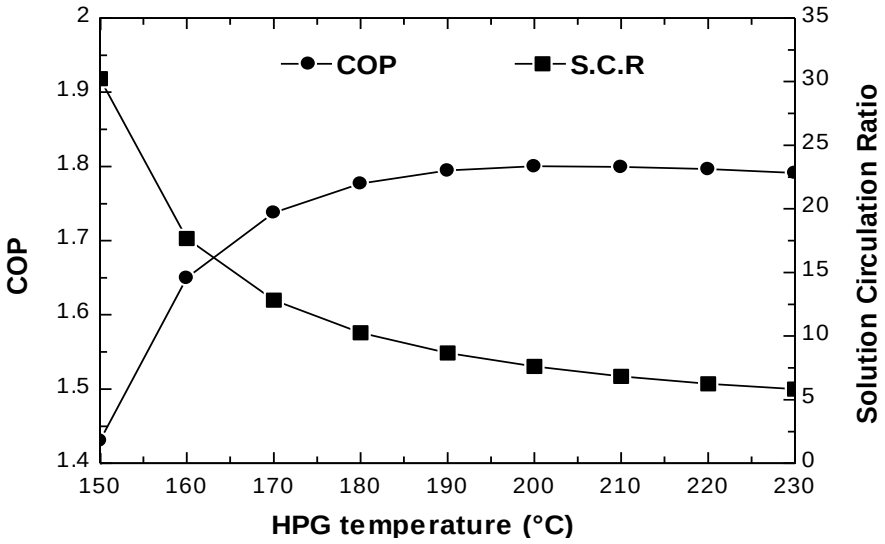

Figure 4. variation of COP and solution circulation ratio at different HPG temperature.

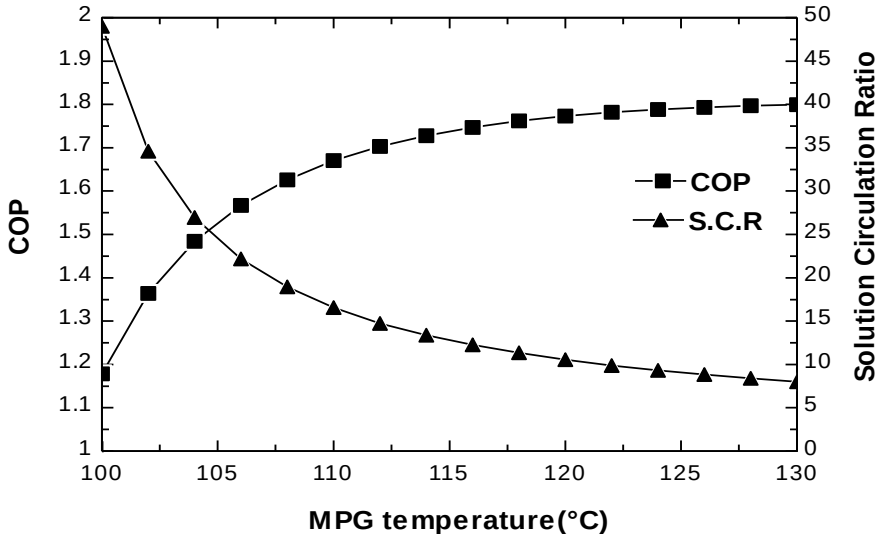

Figure 5. variation of COP and solution circulation ratio at different MPG temperature.

Figure 7. shows variation of LiBr concentration and cooling effect at different LPG temperature. When the LPG temperature increases, concentration of the strong solution in the generator increases, while concentration of the weak solution in the absorber remains constant therefore refrigerant circulation ratio

gradually decreases. The increase in strong solution in the generator should not be excess 70% to prevent the crystallization (solidified) phenomena. This means that the strong solution is limited by the LPG temperature. On the other side, the cooling effect increase with increasing the HPG temperature. In figure 8 shows the variation of the heat loads of generators, condensers and absorber with HPG temperature. As mentioned before, the increase in generators temperature causes the solution circulation ratio to decrease and consequently increases the heat loads of generators, condensers and absorber of the cycle. Figure 9 displays that the system COP is declining with rising the LPC temperature. The refrigerant vapor requires to be cooled for improved condensation processes. In the same figure, the system COP attains his maximum value of 1.86 by decreasing the LPC temperature down to 38°C. On the other side, the circulation ratio increases with increasing the LPC temperature. Figure 10 shows the effect of LPC temperature on cooling capacity of the cycle and LiBr concentration. The cooling capacity drops with increasing LPC temperature. This is because two reasons, the increase in both pressure of LPC and circulation ratio. In the same figure, the strong solution decreases and weak solution increases with increasing of LPC temperature. The effect of heat transfer rates for all components of chiller at different LPC temperature has been shown in Figure 11. All the heat loads decrease when the LPC temperature increase. Figure 12 The influence of the generators temperature on the circulation ratio per unit of cooling capacity. The circulation ratio and cooling capacity decrease with increasing of generators temperature. This implies to reduce this parameter(f/Qe). Figure 13 shows the effect of the evaporator temperature on system COP at different values of HPG temperature. System COP values increase with the increase in evaporator temperature for constant HPG temperature. The effect of evaporator temperature on the system COP values becomes more with an increase in HPG temperature especially at lower values of evaporator temperature.

Figure 14 shows effect of evaporator temperature on cooling capacity of the cycle with different HPG temperature. As the evaporator temperature increases from 5 to 14 C, the cooling capacity of the cycle increases considerably at constant value of HPG temperature. Since the low pressure of the cycle increases as the evaporator temperature increases. In figure 15 shows the variation of the system COP with evaporator temperatures for various the heat exchanger effectiveness. It observed that the system COP increases with the increase of both evaporator temperatures and heat exchanger effectiveness. As the heat exchanger effectiveness increase, the amount of energy adding to the HPG decreases and consequently this improve the system COP.

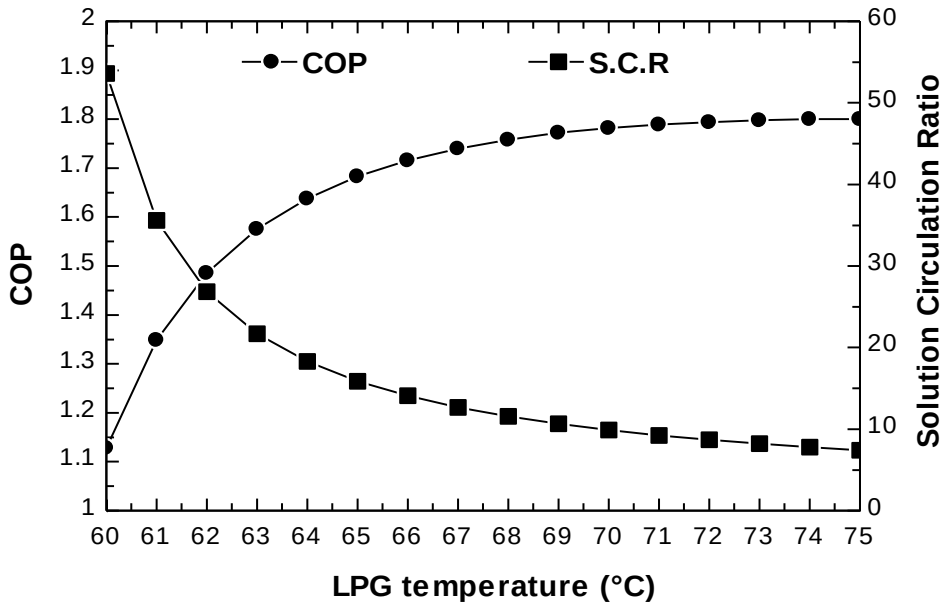

Figure 6. variation of COP and solution circulation ratio at different LPG temperature.

AL-QADISIYAH JOURNAL FOR ENGINEERING SCIENCES

Vol. 10 , No. 2
ISSN: 1998-4456

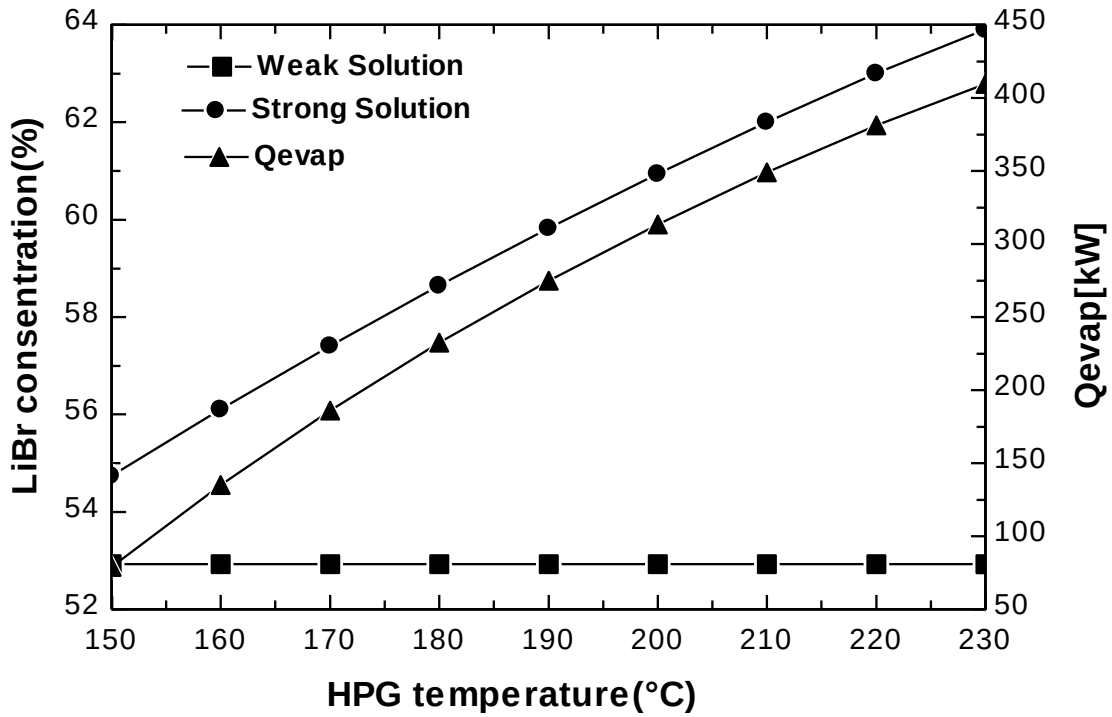

Figure 7. Variation of LiBr concentration and cooling effect at different LPG temperature.

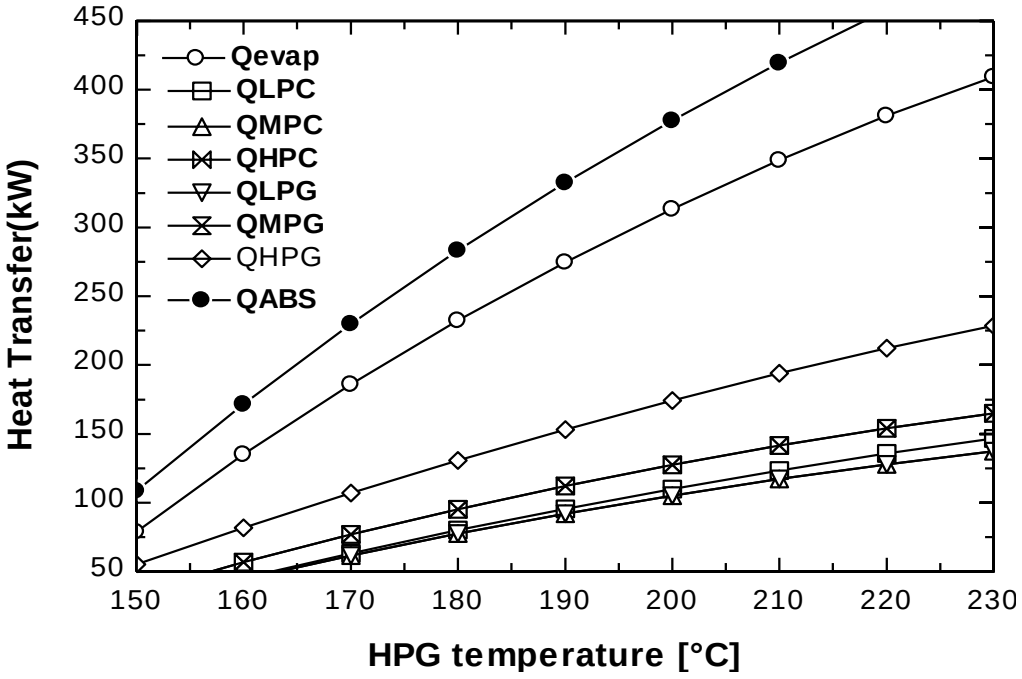

Figure 8. Heat transfer rates for all components of chiller system at different LPG temperature.

AL-QADISIYAH JOURNAL FOR ENGINEERING SCIENCES

Vol. 10 , No. 2
ISSN: 1998-4456

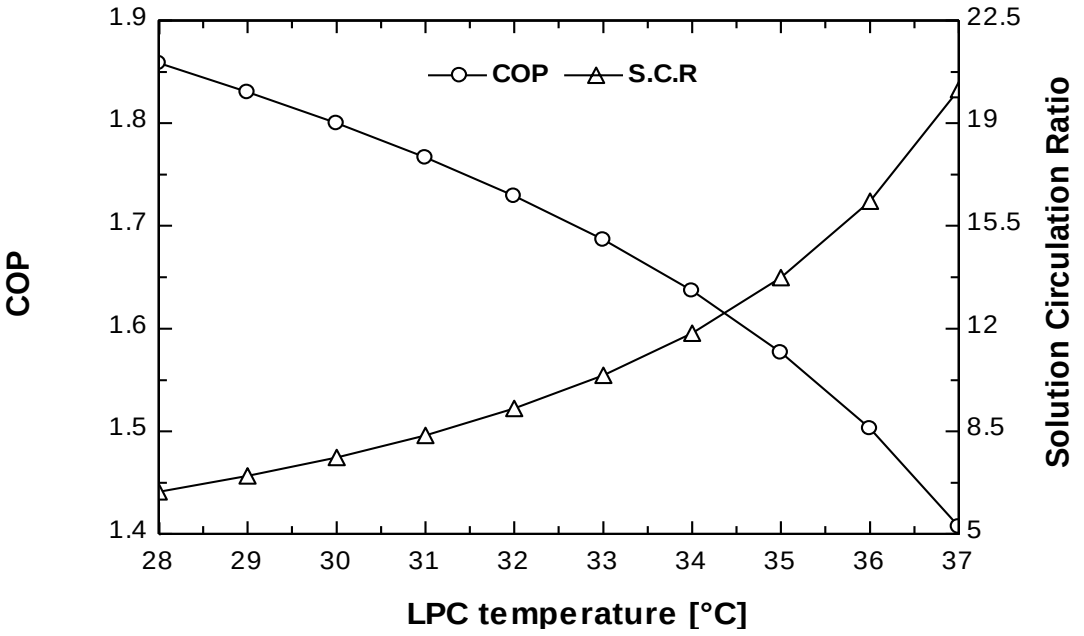

Figure 9. variation of COP and solution circulation ratio at different LPC temperature.

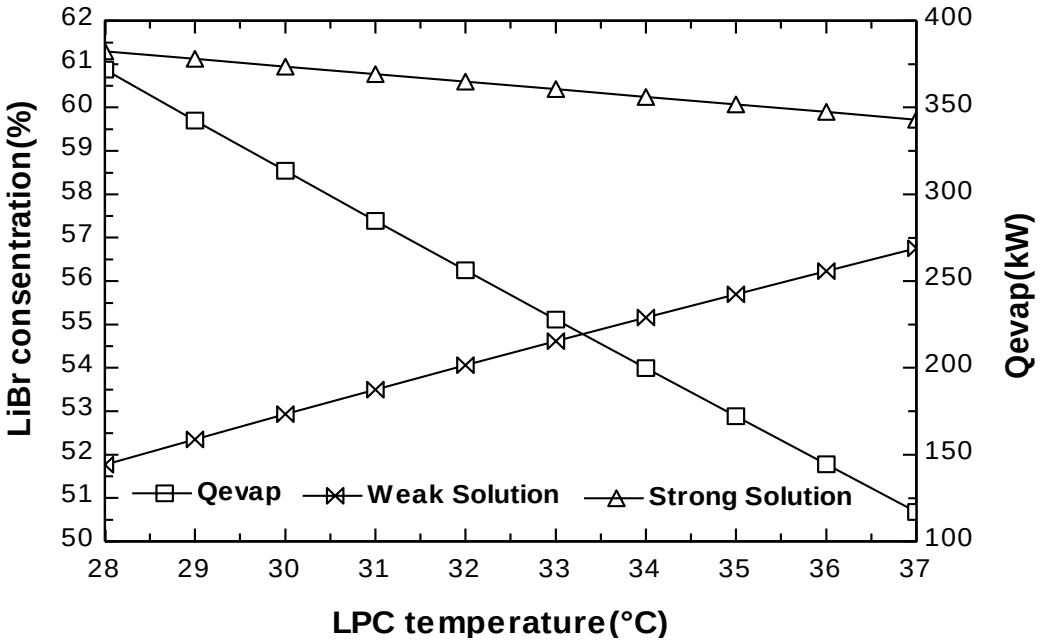

Figure 10. Variation of LiBr concentration and cooling effect at different LPC temperature.

Vol. 10 , No. 2
ISSN: 1998-4456

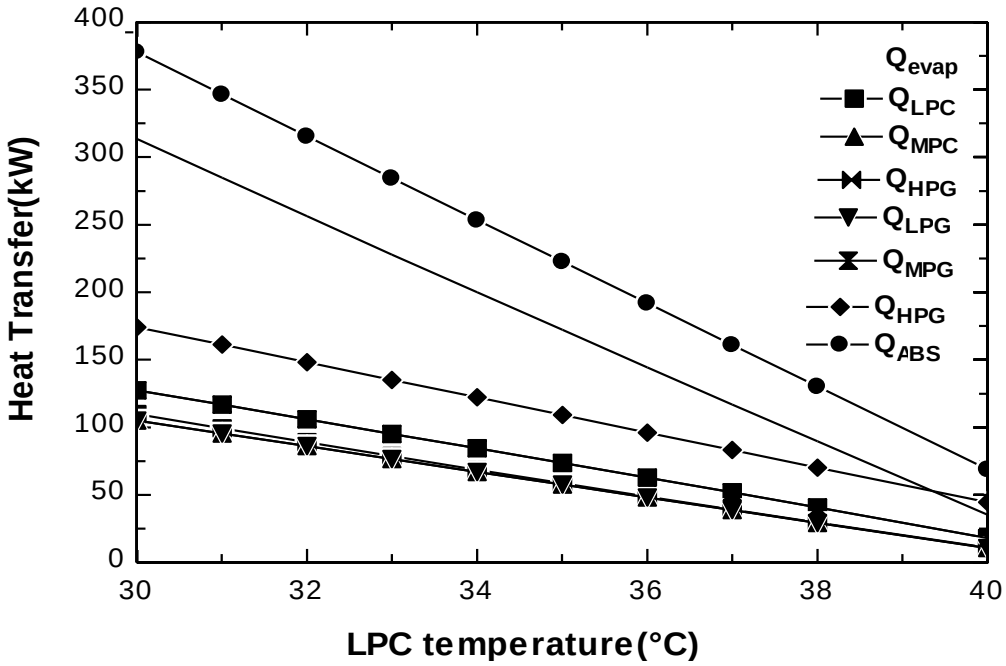

Figure 11. Heat transfer rates for all components of chiller system at different LPC temperature.

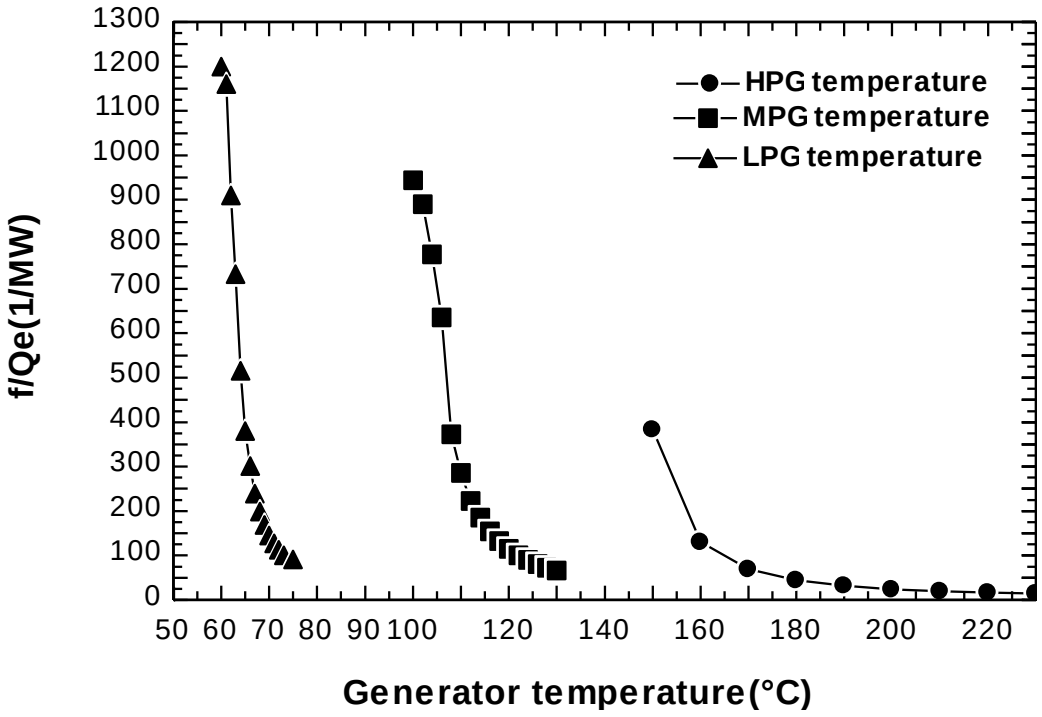

Figure 12. The effect the generators temperature on the circulation ratio per unit of refrigeration load

Vol. 10 , No. 2
ISSN: 1998-4456

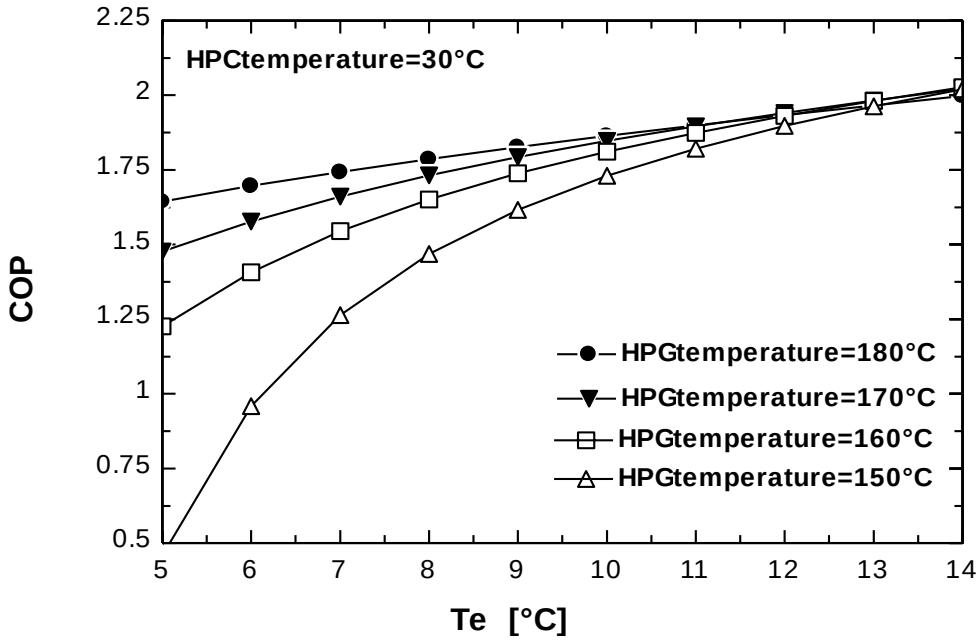

Figure 13. variation of system COP and HPG temperature with different evaporator temperature.

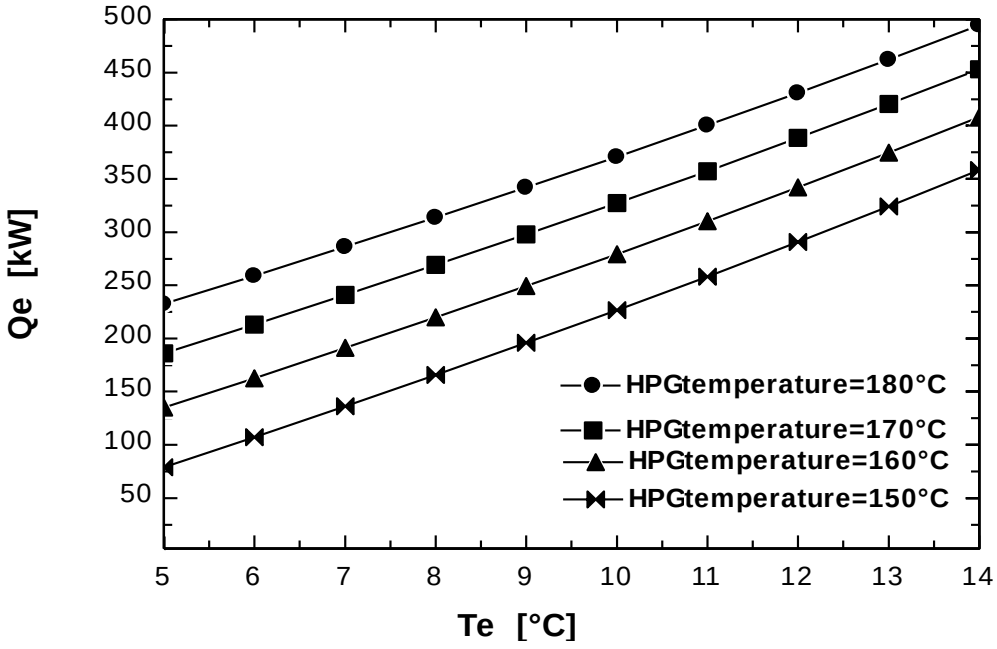

Figure 14. variation of cooling effect and HPG temperature with different evaporator temperature.

AL-QADISIYAH JOURNAL FOR ENGINEERING SCIENCES

Vol. 10 , No. 2
ISSN: 1998-4456

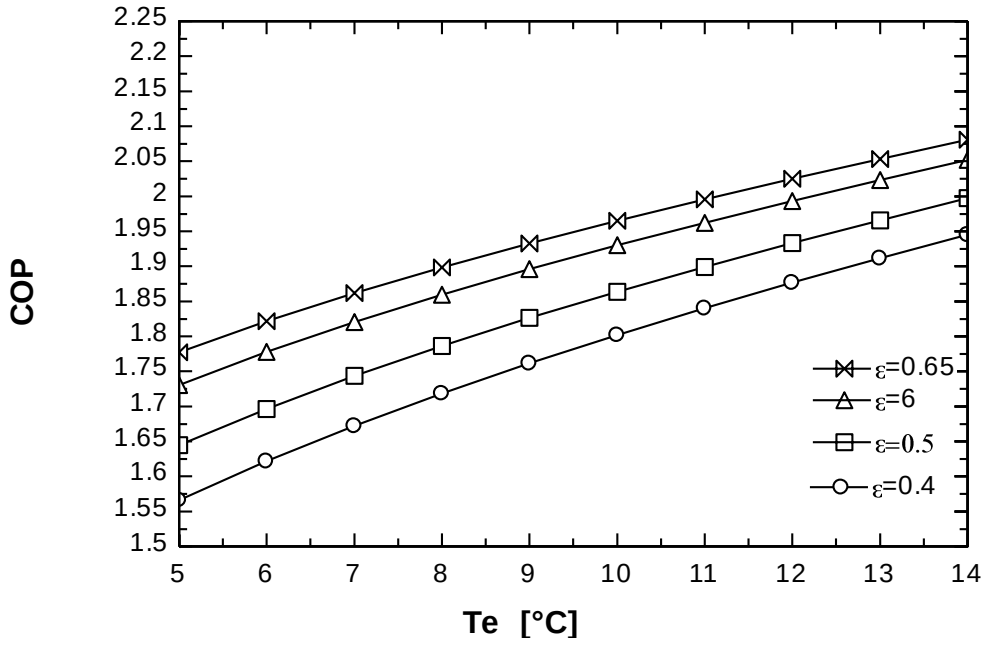

Figure 15. variation of system COP and the heat exchanger effectiveness with different evaporator temperature

CONCLUSION

A computer program written in EES software is modeled for the parametric analysis of triple-stage LiBr-H2O absorption chiller cycle. This cycle is analyzed under steady state operating conditions. The operating parameters are selected as follows: the HPG, MPG and LPG temperatures: THPG= 150-230°C, TMPG= 100-130°C and TLPG= 60-95°C, respectively, LPC temperature TLPC = 28-37°C, evaporator temperature Te = 5-14°C; flow rate of refrigerant mr= 1 kg/s; four values of heat exchangers effectiveness $\varepsilon = 0.4, 0.5, 0.6$ and 0.65. The study leads to the following conclusions:

1- The generators temperature has a strong influence on the performance of the system as well as the condenser temperature. The system COP values increase with increase in HPG, LPG and MPG temperatures. On the other hand, the system COP is declining with rising the LPC temperature.

2- When the LPG temperature increases, concentration of the strong solution in the generator increases, while concentration of the weak solution in the absorber remains constant therefore refrigerant circulation ratio gradually decreases.

3- The increase in generators temperature causes the heat loads of generators, condensers and absorber of the cycle to increase, whereas the increase in LPC temperature implies to decrease the heat loads of the cycle.

4- The cooling capacity of the cycle drops with increasing LPC temperature and rises with increasing LPG temperature.

5- When LPC temperature increases, the strong solution decreases and weak solution increases

6- System COP improves with the increase of both evaporator temperatures and heat exchanger effectiveness for constant HPG temperature.

REFERENCES

1. **Aphornratana Satha and Sriveerakul Thanarath**, 2007, *Experimental studies of a single-effect absorption refrigerator using aqueous lithium–bromide*: Effect of operating condition to system performance, Experimental Thermal and Fluid Science 32, 658–669.

2. **ASHRAE** *fundamentals, Thermodynamic properties of refrigerant*, Chapter 30, Inch-Pound Edition, 2009.

3. **Azhar Md and Siddiqui M. A.**, 2013, *thermodynamic analysis of a gas operated triple effect absorption cycle*, International Journal of Innovative Research in Science, Engineering and Technology Vol. 2, Issue 5.

4. **Bahman Ammar**, 2011, *Modeling of Solar-Powered Single-Effect Absorption Cooling System and Supermarket Refrigeration/HVAC System*, University of South Florida Scholar Commons MSc theses.

5. **Chidambaram LA , Ramana AS , Kamaraj G, Velraj R.**, 2011, *Review of solar cooling methods and thermal storage options*. Renewable and Sustainable Energy Reviews;15:3220–8.

6. **Figueredo Gustavo R., Bourouis Mahmoud, Coronas Alberto**, 2008, *Thermodynamic modelling of a two-stage absorption chiller driven at two-temperature levels*, Applied Thermal Engineering 28 (2008) 211–217.

7. **Florides, G.A., Kalogirou, S.A., Tassou, S.A., Wrobel, L.C**., 2003, *Design and construction of a LiBr–water absorption machine.* Journal of Energy Conversion and Management Vol.44 , Pages 2483–2508.

8. **Gomri, R**., 2009, *Second law comparison of single effect and double effect vapour absorption refrigeration systems*, Energy Conversion and Management, Vol. 50, pp. 1279-1287.

9. **Gomri Rabah**, 2008, *thermodynamic evaluation of triple effect absorption chiller*, Thermal Issues in Emerging Technologies, ThETA 2, Cairo, Egypt, Dec 17-20.

10. **Gomri Rabah**, 2010, *Investigation of the potential of application of single effect and multiple effect absorption cooling systems*, Energy Conversion and Management 51, 1629–1636.

11. **Grossman, G., Zaltash, A.**, 2001, *ABSIM-modular simulation of advanced absorption systems*, International Journal of Refrigeration. Vol. 24 (6), Pages 531–543.

12. **Ha Q.P**, 2013, *A New Single-Effect Hot-Water Absorption Chiller Air Conditioner using Solar Energy*, Australasian Universities Power Engineering Conference.

13**. Hosseini L.**, *Design and Analysis of a Solar Assisted Absorption Cooling System Integrated with Latent Heat Storage*, Master thesis, Delft University of Technology, Holland, 2011.

14. **Joudi, Khalid A., Lafta, Ali H.**, 2001. *Simulation of a simple absorption refrigeration system*. Energy Convers. Manage. 42, Pages 1575–1605.

15. **Karimi, M. N., and S. K. Kamboj**. 2012. "*Exergy Destruction and Chemical Irreversibilities During Combustion in Spark-Ignition Engine Using Oxygenated and Hydrocarbon Fuels*." International Journal of Mechanical & Industrial Engineering 2 (3): 7–11.

16. **Kim, D.S., Infante Ferreira, C.A.**, 2008, *Analytic modelling of steady state single-effect absorption cycles*, International Journal of Refrigeration, 31 (6), 1012-1020.

17. **Klein, S.A**., 2009*. Engineering Equation Solver*, v8.411. F-Chart Software, Madison, Wisconsin.

18**. Marcos J.D., Izquierdo M., Palacios E**., 2011, *New method for COP optimization in water- and air-cooled single and double effect LiBr/water absorption machines*, International Journal of Refrigeration 34, 134 8-1359.

19**. Mehrabian, M.A., Shahbeik, A.E.**, 2005, *Thermodynamic modelling of a single-effect LiBr–H2O absorption refrigeration cycle*. Proc. Inst. Mech. Eng., Part E: J. Process Mech. Eng. Vol. 219 (3), Pages 261–273.

20. **Misra R.D., Sahoo P.K., Gupta A.**, 2005, *Thermoeconomic evaluation and optimization of a double-effect H2O/LiBr vapor-absorption refrigeration system*ll, International Journal of Refrigeration, Vol.28, pp.331-343.

21. **Saghiruddin, M., Siddiqui, A.**, 2001. *Economic analysis of two stage dual fluid absorption cycle for optimizing generator temperatures*. Energy Conv. Manage. 42, 407.

22. **Sencan Arzu, Yakut Kemal A.**, A. *Kalogirou Soteris, Exergy analysis of lithium bromide/water absorption systems*, Renewable Energy 30, 645–657.

23.Source:http://www.thermaxglobal.com/thermax-absorption-cooling-systems/vapour-absorption-machines/steam-fired-chillers/

24. **Somers C. , Mortazavi A. , Hwang Y. , Radermacher R. , Rodgers P. , Al-Hashimi S**.,2011, *Modeling water/lithium bromide absorption chillers in ASPEN Plus*, Applied Energy 88, 4197–4205.

25. **Ullah K.R., Saidur R., Ping H.W., Akikur R.K. , Shuvo N.H**, 2013, *A review of solar thermal refrigeration and cooling methods*, RenewableandSustainableEnergyReviews24, 499–513 .

26**. Wardono, B., Nelson, R**., 1996, *Simulation of Double-effect LiBr/H2O Absorption Cooling System[J]*. ASHRAE J., vol. 38, no.10: p32-38.